Hydrated goethite(α-FeOOH)(100) interface structure: Ordered water and surface functional groups

Sanjit K. Ghose[ab], Glenn A. Waychunas[b], Thomas P. Trainor[c], Peter J. Eng[ad]

[a]Consortium for Advanced Radiation Sources, University of Chicago, Chicago, IL 60637, USA (Corresponding author. Address: Mineral Physics Institute, Stony Brook University, Stony Brook, NY 11794, USA. E-mail address: sghose@bnl.gov
[b]Earth Sciences Division, Lawrence Berkeley National Laboratory, Berkeley, CA 94720, USA
[c]Department of Chemistry and Biochemistry, University of Alaska Fairbanks, Fairbanks, AK 99775-6160, USA
[d]James Franck Institute, University of Chicago, Chicago, IL 60637, USA

Abstract

Goethite(α-FeOOH), an abundant and highly reactive iron oxyhydroxide mineral, has been the subject of numerous studies of environmental interface reactivity. However, such studies have been hampered by the lack of experimental constraints on aqueous interface structure, and especially of the surface water molecular arrangements. Structural information of this type is crucial because reactivity is dictated by the nature of the surface functional groups and the structure or distribution of water and electrolyte at the solid-solution interface. In this study we have investigated the goethite(100) surface using surface diffraction techniques, and have determined the relaxed surface structure, the surface functional groups, and the three dimensional nature of two distinct sorbed water layers. The crystal truncation rod (CTR) results show that the interface structure consists of a double hydroxyl, double water terminated interface with significant atom relaxations. Further, the double hydroxyl terminated surface dominates with an 89% contribution having a chiral subdomain structure on the(100) cleavage faces. The proposed interface stoichiometry is ((H_2O)–(H_2O)–OH_2–OH–Fe–O–O–Fe–R) with two types of terminal hydroxyls; a bidentate (B-type) hydroxo group and a monodentate (A-type) aquo group. Using the bond-valence approach the protonation states of the terminal hydroxyls are predicted to be OH type (bidentate hydroxyl with oxygen coupled to two Fe^{3+}ions) and OH_2 type (monodentate hydroxyl with oxygen tied to only one Fe^{3+}). A double layer three dimensional ordered water structure at the interface was determined from refinement of fits to the experimental data. Application of bond-valence constraints to the terminal hydroxyls with appropriate rotation of the water dipole moments allowed a plausible dipole orientation model as predicted. The structural results are discussed in terms of protonation and H-bonding at the interface, and the results provide an ideal basis for testing theoretical predictions of characteristic surface properties such as pK_a, sorption equilibria, and surface water permittivity.

1. INTRODUCTION

Goethite (α-FeOOH) is one of the most common and reactive crystalline iron oxide phases found in soils and sediments(Cornell and Schwertmann, 2003; van der Zee et al., 2003). Chemical reactions at the goethite/water interface play an important role in numerous natural processes, from controlling the fate and transport of environmental contaminants (Hays et al., 1987; Brown et al., 1999; Cornell and Schwertmann, 2003) to the biological availability and geochemical cycling of iron (Lovley et al., 1991; Lower and Hochella, 2001; Hansel et al., 2004). Because of goethite's importance as a ubiquitous environmental substrate, it is commonly studied to investigate interfacial processes such as sorption, dissolution, aggregation, and precipitation (Sposito, 1989; Davis and Kent, 1990; Brown and Parks, 2001; Brown and Sturchio, 2002; Penn, 2004; Waychunas et al., 2005; Gilbert et al., 2007).

Interfacial processes at model surfaces are frequently studied to understand and interpret many types of macroscopic observations driven by heterogeneous reaction pathways. However, such studies are hampered by the limited molecular knowledge of the aqueous interface structure. Structural information of this type is crucial because reactivity is critically controlled by the precise nature of the surface functional groups and the structure or distribution of water and electrolyte at the solid-solution interface (Hiemstra and Van Riemsdijk, 1996; Hiemstra et al., 1989; Rustad et al., 1996; Sverjensky and Sahai, 1996; Sverjensky, 2005; Sverjensky and Fukushi, 2006; Kubicki et al., 2008). For instance, the widely used surface complexation approach to modeling interfacial reactivity relies on several simplifications and

generalizations about interfacial structure that may result in limited extendibility of model parameters (Davis and Kent, 1990). A number of recent studies have shown that the surface structure of minerals can vary markedly from the bulk stoichiometric termination of the crystal lattice, and that water at the interface may show ordering that is significantly different from bulk water molecular arrangements (Eggleston, 1999; Eng et al., 2000; Cheng et al., 2001; Eggleston et al., 2003; Trainor et al., 2004; Fenter and Sturchio, 2004; Catalano et al., 2007; Tanwar et al., 2007). In several of these cases the differences in reactivity of particular crystal planes can be directly related to the specific surface protonation, functional group occupation, and bond distance relaxations at the surface (Hiemstra and Van Riemsdijk, 1999;Templeton et al., 2001; Bargar et al., 2004).

A considerable amount of both semi-empirical, theoretical and experimental work has gone into development of surface structural and thermodynamic/electrostatic models for goethite-water interfaces (Russel et al., 1974; Parfitt et al., 1975; Hiemstra et al., 1989; Hiemstra et al., 1996; Rustad et al., 1996; Sverjensky and Sahai, 1996; Rakovan et al., 1999; Sverjensky, 2005; Kerisit and Rosso, 2006; Sverjensky and Fukushi, 2006; Kubicki et al., 2008). In many of these efforts, researchers have used structure–reactivity relationships in which an assumed surface structure is used as a starting point for interpreting reactivity, based on the coordination chemistry of surface functional groups. In the majority of these approaches the goethite surface is assumed to be terminated with bulk interatomic distances, site occupations and composition. Purely theoretical approaches to the goethite–water interface have also been attempted, generally assuming a bulk structure surface termination model without a complete aqueous solution in contact with the interface. While the various models have generally proved to have predictive power, and provide a qualitative structural interpretation of reactivity, we know that reduction in surface free energy drives relaxations of near surface atoms, possible deviation of stoichiometry at the surface, and specific surface proton stoichiometry, all of which can have major effects on surface reactivity. Such variations can have significant consequences for the prediction of surface reactivity and chemistry as they can lead to differences in the number and types of reactive sites upon which structure-based reactivity models are founded, as well as substantial differences in local electrostatic interactions affecting proton exchange and hydrolysis (pK_a values). Furthermore, the nature of sorbed water layers may play a significant role in controlling surface processes. Ordering of interfacial water and associated reduction in the interfacial dielectric permittivity may affect sorption behavior markedly. Finally, most experimental work typically utilizes sub-micron sized crystallites that average reactivity over many growth planes and crystallite habits. This approach can only yield incomplete geochemical insight as reactivity is neither connected to an accurate model of interfacial structure, nor is it being observed for a particular set of interfaces.

A number of previous studies have shown ordering of water at crystal/water interfaces (Eng et al., 2000; Cheng et al., 2001; Reedijk et al., 2003; Fenter and Sturchio, 2004; Geissböhler et al. 2004; Toney et al., 1994). In this article we present the experimental determination of the three dimensional atomic structure of goethite/water interface. By use of crystal truncation rod (CTR) analysis we have refined the three-dimensional positions of both surface atoms and overlayer water oxygens (Robinson, 1991; Fenter, 2002; Ghose et al., 2008). Using bond-valence analysis, we have assigned the protonation states of the surface oxygens, from which we can infer the orientation of the surface hydrogen bonding network.

The measurements were performed using a small (100) cleaved crystal from a high quality mineral specimen from Cornwall, UK, resulting in a highly ordered interface that permitted high-resolution structural analysis. The (1 0 0) plane is not the main growth face on natural goethite crystals, but is a common one and the perfect cleavage affords experimental surfaces with no angular miscut. Our analysis provides both the coordination environment of the functional groups terminating the goethite (1 0 0)–water interface as well as the three-dimensional refinement of the overlying water layer molecular positions. The structure refinement shows a double hydroxyl, double water terminated interface with significant atom relaxations. An interesting chiral subdomain structure has also been identified on the (100) cleavage faces. Further, using the structure of the surface hydroxyls and three dimensionally ordered water layers with bond-valence analysis, a complete surface hydroxyl model, along with

dipole orientations of the water layers, could be predicted. These results are useful in comparing and leveraging some of the theoretical models already predicted by DFT calculations, and will also be testable (sorbed water structure and hydroxyl orientations) via sum frequency vibrational spectroscopy (SFVS) measurements.

2. MATERIALS AND METHODS

2.1. Sample preparation

High quality single crystal surfaces of goethite(α-FeO-OH) suitable for CTR diffraction study are uncommon due to the fact that natural samples typically grow as an aggregate of small (<0.1 mm diameter) single and polycrystalline sprays. A natural sample from Cornwall England with crystals up to a millimeter in size provided a rare opportunity to cleave hundreds of small chips that could be sorted optically. Optical and X-ray characterization resulted in about 10 high quality crystals with near atomically smooth cleaved surfaces. All candidates cleaved along the (1 0 0) plane. For this study, we used a chip with a 1 × 1 mm surface, 0.2 mm thickness, that was prepared using an acid–base cleaning procedure and left in water before mounting on the diffractometer in a water saturated He environment (relative humidity >90%, pH_2O > 20 Torr) at standard temperature and pressure condition. (Trainor et al., 2004; Tanwar et al., 2007).

2.2. CTR data collection and data analysis

The data were collected at The University of Chicago Center for Advanced Radiation Sources (CARS), at the Advanced Photon Source (APS) sector 13 undulator beam-line. Experiments were carried out using 12 keV monochromatic X-rays of spot size 50 × 150 μm, from a LN_2 cooled double crystal Si (111) monochromator and using Rh coated vertical and horizontal focusing (and harmonic rejection) mirrors. Sample orientation and scanning were performed using a 2+2+ kappa-geometry diffractometer equipped with a sample cell with X-ray transparent windows (Trainor et al., 2006). To collect non-specular rods the incident angle was fixed at 2° and rocking scans through the truncation rods were performed using a continuous (trajectory) scan of the diffractometer θ-axis at a particular reciprocal lattice setting. Specular rods were collected by scanning the diffractometer ώ-axis with the direction of sample miscut (<0.2°) oriented in the scattering plane to ensure collection of all CTR intensity. A total of 2375 structure factors ($|F_{HKL}|$) were determined by taking the square root of the background subtracted intensity of the rocking scans through the three dimensional crystal truncation rods and correcting for active area, polarization, scan speed, and Lorentz factor (Robinson, 1991). In the notation used above, the reciprocal vector indices H and K correspond to in-plane momentum transfer and L corresponds to perpendicular momentum transfer. After symmetry (*pm*) equivalents were averaged, the final data set consisted of 1760 unique data points from 10 unique crystal truncation rods. The two sigma error bars on the data are typically about 8%. A subset of the data set was recollected periodically to check for beam induced surface damage; these repeats showed 2–5% intensity variation during the course of measurements, which is less than the measurement error, indicating the surface was stable during data collection.

Nonlinear least-squares fits of the full data set to a model consisting of a fixed bulk structure and an adjustable surface region of a-FeOOH (100) were performed using widely used CTR model analysis procedures (Robinson, 1986, 1991; Vlieg, 2000; Fenter, 2002; Trainor et al., 2002; Ghose et al., 2008). The fit parameters include atomic displacements in x, y and z directions, atomic occupancies, Debye–Waller factors, and an overall roughness factor as derived by Robinson (1986). A single overall scale factor was used in the CTR analysis procedure. The quality of the fit is characterized using a reduced χ^2 value. We employed Hamilton's R-ratio test to provide a statistical comparison of the fit quality among different models (Hamilton, 1965). A more detailed discussion of the data analysis procedure is described in a separate file in the Electronic Annex.

2.3. Bond-valence calculation and protonation states

An independent check on the chemical plausibility of the structural models was performed using Pauling's bond-valence (BV) principle (Pauling, 1960), with further quantification using bond strength–bond length relationships as developed by Brown and Altermatt (1985). The Pauling bond-valence sum (s) for a central atom is defined as the sum of individual bond-valence contributions from each neighboring atom, where each contribution is

defined as $s = Z/CN$, where Z is formal valence and CN is the coordination number of the neighboring atom. For accurate comparisons the bond-valences are modified to allow increased s values with shorter interatomic distances and vice versa, and in this way the effects of bond changes due to relaxations or other structural variations can be estimated. This methodology has been shown to be a valuable tool in deducing molecular structural details in the analysis of many of crystal structures, and more recently is finding widespread use in the analysis of surface structures (Hiemstra et al., 1996; Bargar et al., 1997; Venema et al., 1998; Bickmore et al., 2006; Tanwar et al., 2007). In much the same way, using the bond-valence approach the protonation states of the interfacial hydroxyls could be determined by estimating the accepter and donor hydrogen bond contribution to the bond-valence sum in saturating the surface oxygen atoms. In these calculations we assumed that the binding of a single proton to oxygen to form a hydroxyl group contributes approximately 0.8 bond-valence units (vu) to the BV sum, while a hydrogen bond contributes approximately 0.2 vu.

3. RESULTS AND DISCUSSION

3.1. α-FeOOH Bulk and α-FeOOH (1 0 0) surface structure

The bulk goethite(α-FeOOH) structure can be described as a distorted hexagonally close packing of O and OH groups with Fe^{3+} occupying half of the octahedral interstices. Each of the six-coordinated iron sites have three short Fe–O bonds (1.96 Å) and three long Fe–OH bonds (2.10Å) and there are four repeat formula units (FeOOH) present within each unit cell (Fig. 1a) (Cornell and Schwertmann, 2003).The structure has a space group symmetry of *Pnma* and the bulk unit cell parameters are defined in an orthorhombic setting with lattice constants a = 9.9629Å, b = 3.0231Å, and c = 4.6088Å (refined from bulk XRD measurement at The University of Chicago using one of the crystals from the same specimen from which the CTR crystal fragment was obtained). The goethite (1 0 0) surface can be indexed in an orthorhombic setting with the lattice vector c_s defined parallel to the surface normal. This results in a surface unit cell defined by an orthogonal mesh with lattice constants $|a_s|$= 3.0231Å, $|b_s|$= 4.6088Å, and $|c_s|$= 9.9629Å. The (1 0 0) cleavage face of goethite has six chemically distinct terminations of the bulk structure, each occurring with left or right handedness as shown in Fig. 1a: a double hydroxyl layer (layer 1), a single hydroxyl layer (layer 2),an iron over double oxygen layer (layer 3), a double oxygen layer (layer 4), a single oxygen layer (layer 5), and an iron over double hydroxyl layer (layer 6). The presence of the screw axis within the unit cell results in chemically equivalent termination pairs, that have opposite handedness (i.e., layers 1 through 6, left handed, and layers 7–12 right handed) and are therefore crystallographically distinct.

3.2. Surface termination

Nonlinear least-squares fits of the full data set to a model consisting of a fixed bulk structure and an adjustable surface region of a-FeOOH (1 0 0), comprised of thirteen surface layers, were performed. The goodness of the fit was determined from the reduced χ^2. Each of the six distinct terminations was tested, and the double hydroxyl terminated model, (OH)–(OH)–Fe–O–O–Fe–R (R represents the repeat of the stoichiometric atomic layer sequence) was found to be the best fit to the data. A fit of the model with only left handed double hydroxyl termination (layer 1) of the unrelaxed bulk structure resulted in a χ^2 of 7.0 (black dash-dotted lines in Fig. 2). A fit of this model with an equal fraction of the left (layer 1) and right (layer 7) handed terminations, where the surface and near surface atoms, y—z positions, Debye–Waller factors, and occupancies were allowed to vary resulted in a χ^2 value of 3.7 (purple dot dashed lines in Fig. 2). As is evident from the bulk model, any arbitrary x-displacement would deviate from the bulk symmetry. There is no evidence that the surface symmetry deviates from the bulk. Therefore, the x displacements were fixed at their bulk values during the fit. Additional symmetry constraints where used, requiring atoms in symmetry-related domains to maintain the same y and z displacement parameters. Z displacements deeper than eight layers and y displacements deeper than six layers were found to negligibly affect the fit and were therefore fixed at their bulk values in the final analysis (Table1).

The calculated 02L and 22L rods based on the model with equal fractions of opposite handed domains are symmetric about the origin (Fig. 2); however, the data are clearly asymmetric. This indicates that the surface is composed of inequivalent chiral contributions, despite chemical

and energetic equivalency. To better understand the step configuration, atomic force microscopy (AFM) measurements were performed on different cleaved samples (see Electronic Annex for details). Fig. 3a shows atomically flat areas and the existence of a small fraction of steps with heights of quarter, half and three quarters of the unit cell dimension. Half unit cell steps are consistent with the presence of two chiral domains for a given chemical termination, whereas quarter and three quarter steps suggest there is a mixture of chemically distinct domains. These observations lead us to consider a new model with unequal surface fractions for the chemically equivalent but crystallographically distinct terminations in the unit cell.

The CTR data was further refined using a multidomain model (Fig.3b), in which the fractional contribution of the different domains was optimized. The structural parameters for the chiral domains for a given chemical termination are kept the same and only constrained to allow opposing displacement in the *y*-direction. In consideration of possible X-ray coherence length effects, both coherent and incoherent intensity sums from different domains were calculated. The fits are consistently of higher quality using the incoherent summation method. Hence, subsequent intensities summation was done in-coherently during the rest of the fitting process. This new multidomain model improves the fit at the 95% confidence level by Hamilton's test (Hamilton, 1965), yielding a χ^2 value of 2.53 (Fig. 4, blue solid line). The best fit model consists of 71% double hydroxyl layer 1, 9% double oxygen layer 4, 18% double hydroxyl layer 7 (the opposite handed layer 1) and 2% double oxygen layer 10 (the opposite handed layer 4, Fig. 1a) with the layer fractions determined with a 2% uncertainty (Fig. 3b).We note that the double hydroxyl terminated surface dominates with an 89% contribution. Heterogeneity in surface step morphology has been reported on cleaved goethite crystals previously (Rakovan et al., 1999). This may be due to stress variations as a fracture propagates through the crystal, analogous to the chirality of $K_2Cr_2O_7$ surface domains which have been shown to be controlled by the direction of cleavage forces (Plomp et al., 2001).

3.3. Interface structure

Although the multidomain model yields reasonable FeAOH bond lengths and plausible chemical coordination for the terminal Fe atoms, close examination shows misfits to the (00L) and (H0L) rod data (Fig. 4). The good fit to rods with large in-plane momentum transfer together with the pronounced misfit on the 00*L* rod (specular at *L* = 1.5, 2.5 and *L* = 6.75) and 10L low Q in-plane rods, indicates there is a missing component in the model with substantial in-plane disorder. To address this we added a single layer of oxygen (W_1, Fig. 1a) with its own displacement and disorder parameters to the model, intended to simulate a partly ordered hydrogen-bonded water layer. The water layer was added to all the chemically and crystallographically different domains starting at their bulk oxygen positions. During subsequent fitting only the parameters of this new oxygen layer (W_1) were allowed to vary resulting in a χ^2 value of 2.19, an improvement at the 95% confidence level (Hamilton, 1965). The in and out of plane displacement of the first oxygen layer (W_1) with a Debye–Waller factor (DWF) of 4Å^2 resulted in a good fit to the specular and low Q off-specular rods (Fig. 4). However, at *L* =3 on the (00L) rod a small misfit remained (green solid line, Fig.4) prompting the addition of a second oxygen layer (*W*2, Fig.1a) with separate displacement, disorder and occupancy parameters. This model was tested with both oxygen (waters *W*1, *W*2) layers and the terminal hydroxyls free to move during optimization. The double oxygen overlayer model (Fig.1a and b) produced our best fit (red solid line Fig. 2 & Fig. 4) with $\chi^2 = 2.11$ (an improvement at the 95% confidence level).

A striking feature of the water layers is their three dimensional order. Based on the DWF and the estimated errors (see Table 1), W_1 water is well ordered both in and out of plane. In comparison, W_2 water has substantial out of plane ordering with its in-plane coordinates less certain indicating greater in-plane disorder than W_1. Both the W_1 and W_2 water layers are uniquely constrained in the *x* and *z* directions, and positioned 1.9Å and 3.3Å above the layer 1 oxygen respectively. There is, however, degeneracy in the *y*-direction since a model with *y* positions swapped between the W_1 and W_2 water layer gives an equally good fit. We selected the solution that is most plausible both sterically and with respect to formation of hydrogen bonds with the terminal hydroxyls. The three dimensional ordering of the water layers appears to be similar to previous theoretical simulations and experimental findings (Toney et al, 1994; Eng et al., 2000; Cheng et al., 2001; Reedijk

et al., 2003; Fenter and Sturchio, 2004; Ostroverkhov et al., 2005; Kerisit and Rosso, 2006). The occupancy of the W_1 and W_2 layers yields 1.4 ± 0.2 waters per surface unit cell (see Table 1). The O–O distance between W_2 and terminal hydroxyl layers ^{I}O and ^{II}O are 3.46 ± 0.07Å and 4.19 ± 0.05Å, respectively, and the distance between W_1 and terminal hydroxyl layers ^{I}O and ^{II}O are 2.97 ± 0.04Å and 2.49 ± 0.02Å, respectively. Based on these O–O distances we conclude there are apparently two distinct types of water-surface interactions: W_1 is likely hydrogen bonding to the terminal hydroxyl groups (e.g., in the bulk the O–H...O distance is 2.76Å (Cornell and Schwertmann, 2003)), while W_2 does not have direct interaction with terminal hydroxyl groups, and is interacting most strongly with the W_1 waters (Fig.5).

Table 1 compares the best fit and the unrelaxed double hydroxyl surface model. The fit model indicates that near surface Fe^{3+} are six-coordinated and connect to two types of surface (hydr)oxo groups: monodentate (Fe–O) (A-type) and bidentate (Fe_2O) (B-type)(Fig.1a). Despite large *y*-relaxations and interlayer contractions for layers 1–2 and expansions for layers 2–3, the surface Fe–hydroxyl bond lengths are 2.16 ± 0.03Å and 2.09 ± 0.03Å, close to the bulk value of 2.10Å. The occupancies of the Fe, ^{I}O and ^{II}O layers, track within error, hence maintaining a fixed Fe/O ratio. An rms surface roughness of 1.8 ± 0.4Å determined from the CTR measurement is consistent with the AFM measurement, indicating a relatively smooth surface.

3.4. Interfacial hydroxyl structure

Hydrogen positions cannot be directly fit in our model due to their relative weak X-ray scattering factors. However, protonation states of surface oxygens may be estimated from the number of hydroxyl bonds and/or hydrogen bonds required to satisfy oxygen bond-valence sum. The Fe–O bond-valence contributions were computed using the bond length–bond strength relationships of Brown and Altermatt (1985). The results (Table1) show that the uppermost Fe layer has a BV sum of 2.95 ± 0.04 valence units (vu), identical to the bulk value of 2.96 vu, indicating reasonable Fe^{3+} coordination. The terminal oxygen atoms have a BV sum of 0.34 ± 0.06 vu and 0.82 ± 0.04 vu for layer 1 (^{I}O) and layer 2 (^{II}O), respectively (Fig 1a), showing substantial undersaturation. Following numerous studies, we assume that adding a proton to form a hydroxyl group contributes approximately 0.8 vu to the BV sum, while a hydrogen bond contributes approximately 0.2 vu (Brown and Altermatt, 1985). The addition of one proton results in BV sums of 1.14 ± 0.06 vu, and 1.62 ± 0.04 vu for layer 1 (^{I}O) hydroxyl, and layer 2 (^{II}O) hydroxyl, respectively. The layer 1 oxygen is thus near saturation of 2 vu with the addition of a second proton ($–OH_2$), but addition of a second proton to the layer 2 oxygen results in substantial oversaturation. Hence we assign these oxygens to be doubly and singly protonated, respectively. Addition of a single hydrogen bond to layer 2 oxygen yields a sum of 1.82 vu slightly undersaturated, but another bond is unlikely due to steric constraints.

Considering the bond-valence sums and steric factors, it is inferred that the $Fe–OH_2$ surface sites should be H-bond donors while the $Fe_2–OH$ sites act as H-bond acceptors and donors (Venema et al., 1998). The assignment of the layer 1 oxygens as aquo groups, of the form $Fe–OH_2$, based on BV is also consistent with the refined structural parameters. We observe a large disorder parameter (DWF, Table1) for the layer 1 (^{I}O) hydroxyls consistent with a (loosely bound) singly coordinated surface species. Given this likely weak binding, and the proximity (and high disorder) of the W_2 water groups, it is plausible that these sites participate in dynamic exchange (Casey et al., 2000; Phillips et al., 2000). This proton configuration results in $Fe–OH_2$ and $Fe_2–OH$ groups being the dominant moieties exposed at the α-FeOOH (100) surface. This same stoichiometry was suggested by Kubicki et al. (2008) to be the lowest energy surface based on their ab initio calculations.

From the CTR model and BV analysis we infer that the layer 1 oxygen is saturated by double protonation. Layer 2 oxygen is singly protonated and could be saturated with a hydrogen bond to layer W_1 water. The orientations of the water molecules were inferred by only considering configurations that satisfy the bond-valence requirements while maintaining a tetrahedral coordination of the oxygens. With the above constraints a plausible hydrogen bonding network could be described with the dipoles of the water layers oriented such that layer 1 oxygen attains a near valence saturation (2 vu) and oxygen of W_1 water layer builds a tetrahedral co-ordination with water layers above (Fig. 5). The average O–O distance within the ordered water (W_1–W_2) is 2.68

± 0.03Å, shorter than that in liquid water, but similar to that found in the orthorhombic ice XI structure (2.73Å) (Line and Whitworth, 1996).

The above defined water model and H-bonding network also suggests a well defined orientation of the water dipoles (Fig. 5). The interfacial dielectric properties and water mobility will be influenced by the orientation of the water molecules and the structure of the H-bonding network. As water ordering is coupled to the domain model, the net handedness of this domain arrangement leads to a net in-plane water dipole moment. This net moment is expected to be experimentally verifiable using sum frequency vibrational spectroscopy (SFVS) (Ostroverkhov et al., 2005). The water orientation should also be strongly influenced by the surface charge; the current model proposes that the layer 1 oxygen is doubly protonated, hence the surface carries a net positive charge. Therefore, the negative water dipoles are facing the doubly protonated surface positive charge. Deprotonation of this group at higher pH (Venema et al., 1998) would likely alter the water arrangement significantly. The water model presented in this study differs slightly from that suggested by Kubicki et al. (2008) in their DFT calculations for a neutral surface. However, as we expect that under the circum neutral pH conditions of the experiment there is a net positive surface charge, differences in hydrogen bond lengths and dipole orientation are expected. In our model the W_1 water layer acts as a proton donor and acceptor with the surface hydroxyls forming H-bonds of 2.0Å and 1.7Å with Fe–OH_2 and Fe_2–OH surface functional groups (Fig. 5), respectively. Kubicki et al. in their DFT calculation reported these two H-bonds to be 1.6Å and 1.55Å for the L_1 water layers to the surface hydroxyls. The H-bond lengths decide the bonding strength and dipole orientation of the adsorbed water layers with respect to the surface hydroxyls.

3.5. Reactivity of interfacial hydroxyls

The posited interface structure allows testing of structure-based reactivity models and their sensitivity to choice of surface termination and stoichiometry. For example, Bronsted acidity of the surface (hydr)oxo groups, expressed in terms ofpKa values, can be estimated from a semi-empirical model. The CD-MUSIC (Hiemstra et al., 1989) model uses a surface (hydr)oxo group's BV sum for the prediction of site pKa values. This model predicts a first pK_a value of 7.7 for a $FeOH_2$ (presumably with single hydroxyl and single hydrogen bond) group using a Fe–O BV contribution of 0.61 vu (Venema et al., 1998). However the Fe–O bond length for the doubly protonated surface group in our model results in a significantly lower BV of 0.34 vu which suggests a different pK_a value. However, deprotonation of this group should result in bond length contraction and increased stability of the FeOH group (Bargar et al., 1997). Our analysis shows that a semi-empirical BV approach may be compromised by using bulk metal-oxygen bond lengths because: (1) actual bond lengths will depend upon both protonation state and nature of hydrogen bonding, and (2) feedback between surface relaxation and site saturation is ignored by using bulk bond lengths.

Summarizing, we propose the interface stoichiometry to be ((H_2O)–(H_2O)–OH_2–OH–Fe–O–O–Fe–R) with two types of terminal hydroxyls; a bidentate (B-type) hydroxo group and a monodentate (A-type) aquo group. These functional groups provide effective Lewis base sites for cations through direct inner-sphere association (Arai et al., 2001) of Lewis acids (e.g., via proton exchange). The high lability of the A-type aquo group would also result in an effective Lewis Base exchange site. These aquo groups may also be effective sites for strong Coulombic association with anions species, due to their excess positive charge, and hence result in effective outer sphere binding of species such as arsenate (Catalano et al., 2008).

4. CONCLUSIONS

The interface molecular structure of goethite (100)/ water has been determined using CTR and bond-valence analysis methods. The interface structure is determined as a double hydroxyl, double water terminated interface with significant atom relaxations. Further, the double hydroxyl terminated surface dominates with an 89% contribution havinga chiral subdomain structure on the (1 0 0) cleavage faces. The proposed interface stoichiometry is ((H_2O)–(H_2O)–OH_2–OH–Fe–O–O–Fe–R) with two types of terminal hydroxyls; a bidentate (B-type) hydroxo group and a monodentate (A-type) aquo group. Using the bond-valence approach we determined the protonation states of the terminal hydroxyls to be OH type (bidentate hydroxyl with oxygen coupled to two Fe^{3+} ions) and OH_2 type (monodentate hydroxyl

with oxygen tied to only one Fe^{3+}). A double layer three dimensional ordered water structure at the interface was determined from refinement of fits to the experimental data. Further, application of bond-valence constraints to the terminal hydroxyls with appropriate rotation of the water dipole moments allowed a plausible dipole orientation model to be predicted. The overall analysis clarifies how the ordered water structure and dipole orientations are derived by a combination of the surface structure and specific charge/protonation state of the terminal hydroxyls. From the protonation models of the interfacial hydroxyls, the relative Bronsted acidity of the surface (hydr)oxo groups, generally expressed in terms of surface pK_a value(s) could be estimated using a semi-empirical approach. Finally, the experimental results for the interfacial hydroxyls and their protonation state could be useful as a direct comparison with theoretical and computational predictions made by previous studies.

Numerous studies have utilized goethite as a model environmental sorbent and data interpretation requires assumptions about the surface chemistry, sorbate binding, and magnitude of binding constants. Our results provide a detailed interface structural model that removes many of these assumptions. Hence our findings have direct implications for site-specific models of proton and metal–ion sorption at the goethite (1 0 0) water interface. Further, many of the structure and bonding ideas treated here will also apply to sorption of any species on goethite surfaces, and may be generalizable to other environmental oxides.

ACKNOWLEDGMENTS

The authors thank Lahsen Assoufid, Sarah Petitto, Kunaljeet Tanwar, Jeffry G. Catalano and Joseph Pluth, for their help at different stages of the work. Our thanks also go to Prof. Gordon E. Brown Jr. for his useful and insightful discussion. We also appreciate and thank four anonymous reviewers and the Associate Editor K. Rosso for their constructive comments and suggestions. This research was supported by NSF-NIRT (NSF-0404400) and NSF-EMSI (NSF-0431425) Grants and the Director, Office of Science, Office of Basic Energy Sciences, Division of Chemical Sciences, Geosciences, and Biosciences, of the U.S. Department of Energy under Contract No. DE-AC02-05CH11231. The measurements are done at GeoSoilEnviroCARS (Sector 13) of the Advanced Photon Source (APS), Argonne National Laboratory. GeoSoilEnviroCARS is supported by the National Science Foundation–Earth Sciences EAR-0622171 and Department of Energy Geosciences DE-FG02-94ER14466. Use of the APS was supported by DOE, Office of Science, and Office of Basic Energy Sciences, Office of Energy Research, under Contract No. DE-AC02-06CH11357.

APPENDIX A. SUPPLEMENTARY DATA

Supplementary data associated with this article can be found, in the online version, at doi:10.1016/j.gca.2009.12.015.

REFERENCES

Arai Y., Elzinga E. J. and Sparks D. L. (2001) X-ray absorption spectroscopic investigation of arsenite and arsenate adsorption at the aluminum oxide–water interface. J. Colloid Interface Sci. 235, 80–88.

Bargar J. R., Towle S. N., Brown, Jr., G. E. and Parks G. A. (1997) XAFS and bond-valence determination of the structures and compositions of surface functional groups and Pb(II) and Co(II) sorption products on single-crystal α-$A_{l2}O_3$. J. Colloid Interface Sci. 185, 473–492.

Bargar J. R., Trainor T. P., Fitts J. P., Chambers S. A. and Brown, , G. E. (2004) In situ grazing-incidence extended X-ray absorption fine structure study of Pb(II) chemisorption on hematite (0001) and (1–102) surfaces. Langmuir 20, 1667– 1673.

Bickmore B. R., Rosso K. M., Tadanier C. J., Bylaska E. J. and Doud D. (2006) Bond-valence methods for pKa prediction. II. Bond-valence, electrostatic, molecular geometry, and solvation effects. Geochim. Cosmochim. Acta 70, 4057–4071.

Brown, Jr., G. E., Henrich V. E., Casey W. H., Clark D. L., Eggleston C., Felmy A., Goodman D. W., Gratzel M., Maciel G., McCarthy M. I., Nealson K. H., Sverjensky D. A., Toney M. F. and Zachara J. M. (1999) Metal oxide surfaces and their interactions with aqueous solutions and microbial organisms. Chem. Rev. 99, 77–174.

Brown, Jr., G. E. and Parks G. A. (2001) Sorption of trace elements on mineral surfaces: Modern perspectives from spectroscopic studies, and comments on sorption in the marine environment. Int. Geol. Rev. 43, 963–1073.

Brown, Jr., G. E. and Sturchio N. C. (2002) Applications of synchrotron radiation in low-temperature geochemistry and environmental sciences. Rev. Min. Geo Chem 49, 1–115.

Brown I. D. and Altermatt D. (1985) Bond-valence parameters obtained from a systematic analysis of the inorganic crystal structure database. Acta Crystallogr. B Struct. Sci. 41, 244–247.

Casey W. H., Phillips B. L., Karlson M., Nordin S., Nrodin J. P., Sullivan D. J. and Crawford S. N. (2000) Rates and mechanisms of oxygen exchanges between sites in the AlO_4A-$l_{12}(OH)_{24}(H_2O)_{12}^{7+}$(aq) complex and water: implications for mineral surface chemistry. Geochim. Cosmochim. Acta 64, 2951–2964.

Catalano J. G., Fenter P. and Park C. (2007) Interfacial water structure on the (0 1 2) surface of hematite: ordering and reactivity in comparison with corundum. Geochim. Cosmochim. Acta. 71, 5313–5324.

Catalano J. G., Park C., Fenter P. and Zhang Z. (2008) Simultaneous inner-and outer-sphere arsenate adsorption on corundum and hematite. Geochim. Cosmochim. Acta. 72, 1986– 2004.

Cheng L. X., Fenter P., Nagy K. L., Schlegel M. L. and Sturchio

N. C. (2001) Molecular-scale density oscillations in water adjacent to a mica surface. Phys. Rev. Lett. 87, 156103-1– 156103-4.

Cornell R. M. and Schwertmann U. (2003) The iron oxides: structure, properties, reactions, occurrence and uses. Wiley-VCH, Weinheim.

Davis J. A. and Kent D. B. (1990) Surface complexation modeling in aqueous geochemistry. In Mineral-Water Interface Geochemistry, 23 (eds. M. F. Hochella Jr. and A. F. White). Rev. Mineral., pp. 177–260.

Eggleston C. M., Stack A. G., Rosso K. M., Higgins S. R., Bice A. M., Boese S. W., Pribyl R. D. and Nichols J. J. (2003) The structure of hematite (α-Fe_2O_3) (0 0 1) surfaces in aqueous media: scanning tunneling microscopy and resonant tunneling calculations of coexisting O and Fe terminations. Geochim. Cosmochim. Acta 67, 985–1000.

Eggleston C. M. (1999) The surface structureof a-Fe2O3(001)by scanning tunneling microscopy (STM): Implications for electron transfer reactions. Am. Mineral. 84, 1061–1070.

Eng P. J., Trainor T. P., Brown, Jr., G. E., Waychunas G. A., Newville M., Sutton S. R. and Rivers M. L. (2000) Structure of the hydrated a-Al2O3(0001) surface. Science 288, 1029–1033.

Fenter P. and Sturchio N. C. (2004) Mineral-water interfacial structures revealed by synchrotron X-ray scattering. Prog. Surf. Sci. 77, 171–258.

Fenter P. (2002) Applications of synchrotron radiation in low-temperature geochemistry and environmental sciences. Rev. Min. Geo Chem. 49, 149–216.

Geissbuhler P., Fenter P., DiMasi E., Srajer G., Sorensen L. B. and SturchioN.C. (2004) Three-dimensional structure of the calcite–water interface by surface X-ray scattering. Surf. Sci. 573, 191–203.

Ghose, S.K., Tanwar, K., Petitto, S., Lo, C.S., Eng, P.J., Trainor, T.P., and Chaka, A.M., (2008). Developments in Earth & Environmental Sciences: Adsorption of Metals by Geomedia II; Elsevier: Amsterdam, 2008, 7, pp. 1–24.

Gilbert B., Lu G. and Kim C. S. (2007) Stable cluster formation in aqueous suspensions of iron oxyhydroxide nanoparticles. J. Colloid Interface Sci. 313, 152–159.

Hamilton W. C. (1965) Significance tests on crystallographic R factor. Acta Crystallogr. 18, 502–510.

Hansel C. M., Benner S. G., Nico P. and Fendorf S. (2004) Structural constraints of ferric(hydr)oxides on dissimilatory iron reduction and the fate of Fe(II). Geochim. Cosmochim. Acta. 68, 3217–3229.

Hays K. F., Roe A. L., Brown, Jr., G. E., Hodgson K. O., Leckie J. O. and Parks G. A. (1987) In-situ X-ray absorption study of surface complexes: selenium oxyanions on a-FeOOH. Science 238, 783–786.

Hiemstra T. and Van Riemsdijk W. H. (1996)A surface structural approach to ion adsorption: the charge distribution (CD) model. J. Colloid Interface Sci. 179, 488–508.

Hiemstra T., de Wit J. C. M. and Van Riemsdijk W. H. (1989) Multisite proton adsorption modeling at the solid/solution interface of (hydr)oxides: a new approach II. Application to various important (hydr)oxides. J. Colloid Interface Sci. 133, 105–117.

Hiemstra T. and Van Riemsdijk W. H. (1999) Effect of different crystal faces on experimental interaction form and aggregation of hematite. Langmuir 15, 8045–8051.

Hiemstra T., Venema P. and Van Riemsdijk W. H. (1996) Intrinsic proton affinity of reactive surface groups of metal (hydr)oxides: the bond valence principle. J. Colloid Interface Sci. 184, 680–692.

Kerisit S. and Rosso K. M. (2006) Computer simulation of electron transfer at hematite surfaces. Geochim. Cosmochim. Acta 70, 1888–1903.

Kubicki J. D., Paul K. W. and Sparks G. L. (2008) Periodic density functional theory calculationsof bulk and the (010) surface of goethite. Geochem. Trans. 9, 1–16.

Line M. B. C. and Whitworth R. W. (1996) A high resolution neutron powder diffraction study of D_2O ice XI.J. Chem. Phys. 104, 10008–10013.

Lovley D. R., Phillips Ellzabeth J. P. and Lonergan D. L. (1991) Enzymatic versus nonenzymatic mechanisms for Fe(III) reduction in aquatic sediments. Environ. Sci. Technol. 25, 1062–1967.

Lower S. K., Hochella M. F. and Beveridge T. J.

(2001) Bacterial Recognition of Mineral Surfaces: nanoscale interactions between Shewanella and a-FeOOH. Science 292, 1360–1363.

Ostroverkhov V., Waychunas G. A. and Shen Y. R. (2005) New information on water interfacial structure revealed by phase-sensitive surfacespectroscopy. Phys. Rev. Lett. 94, 46102–46104.

Parfitt R. L., Russel J. D. and Farmer V. C. (1975) Confirmation of the surface structure of goethite (a-FeOOH., phosphated goethite by infrared spectroscopy. Soil Sci. Soc. Am. Proc. 39, 1082–1087.

Pauling L. (1960) The Nature of the Chemical Bond, third ed. Cornell University Press, Cornell.

Penn R. L. (2004) of Oriented Aggregation. J. Phys. Chem. B 108, 12707–12712.

Phillips B. L., Casey W. H. and Karlson M. (2000) Bonding and reactivity at oxide mineral surfaces from model aqueous complexes. Nature 404, 379–382.

Plomp M., van Enckevort W. J. P. and Vlieg E. (2001) Controlling crystal surface termination by cleavage direction. Phys. Rev. Lett. 86, 5070–5072.

Rakovan J., Becker U. and Hochella, Jr., M. F. (1999) Aspects of goethite surface microtopography, structure, chemistry, and reactivity. Am. Miner. 84, 884–894.

Reedijk M. F., Arsic J., Hollander F. F. A., de Vries S. A. and Vlieg E. (2003) Liquid order at the interface of KDP crystals with water: evidence for icelike layers. Phys. Rev. Lett. 90, 66103.

Robinson I. K. (1991) Surface Crystallography. In In Handbook on Synchrotron Radiation, vol. 3 (eds. G. S. Brown and D. E. Moncton). Elsevier, North-Holland:Amsterdam, pp. 221–226.

Robinson I. K. (1986) Crystal truncation rods and surface roughness. Phys. Rev. B 33, 3830–3836.

Rustad J. R., Felmy A. R. and Hay B. P. (1996) Molecular statics calculations for iron oxide and oxyhydroxide minerals: toward a flexible model of the reactive mineral-water interface. Geochim. Cosmochim. Acta. 60, 1563–1576.

Russel J. D., Parfitt R. L., Fraser A. R. and Farmer V. C. (1974) Surface structure of gibbsite, goethite and phosphated goethite. Nature 248, 220–221.

Sposito G. (1989) Surface reactions in natural aqueous colloidal systems. Chimica 43, 169–176.

Sverjensky D. A. (2005) Prediction of surface charge on oxides in salt solutions: revisions for 1:1 (M_L_) electrolytes. Geochim. Cosmochim. Acta 69, 225–257.

Sverjensky D. A. and Sahai N. (1996) Theoretical prediction of single-site surface-protonation equilibrium constants for oxides and silicates in water. Geochim. Cosmochim. Acta 60, 3773–3798.

Sverjensky D. A. and Fukushi K. (2006) Anion adsorption on oxide surfaces: inclusion of the water dipole in modeling the electrostatics of ligand exchange. Environ. Sci. Technol. 40, 263–271.

Tanwar K. S., Lo C. S., Eng P. J., Catalano J. G., Walko D. A., Brown, Jr., G. E., Waychunas G. A., Chaka A. M. and Trainor T. P. (2007), Surface diffraction study of the hydrated hematite (102) surface. Surf. Sci. 601, 460–474.

Templeton A. S., Trainor T. P., Traina S. J., Spormann A. M. and Brown, Jr., G. E. (2001) Pb(II) distributions at biofilm-metal oxide interfaces. Proc. Nat. Acad. Sci. 98, 11897–11902.

Toney M. F., Howard J. N., Richer J., Borges G. L., Gordon J. G., Melroy O. R., Wiesler D. G., Yee D. and Sorensen L. B. (1994) Voltage-dependent orderung of water molecules at an electrode-electrolyte interface. Nature 368, 444–446.

Trainor T. P., Chaka A. M., Eng P. J., Newville M., Waychunas G. A., Catalano J. G. and Brown, Jr., G. E. (2004) Structure and reactivityof the hydrated hematite(0001) surface. Surf. Sci. 573, 204–224.

Trainor T. P., Templeton A. S. and Eng P. J. (2006) Structure and reactivity of environmental interfaces: application of grazing angle X-ray spectroscopy and long-period X-ray standing waves. J. Electron. Spectrosc. Relat. Phenom. 150, 66– 85.

Trainor T. P., Eng P. J. and Robinson I. K. (2002) Calculation of crystal truncation rod structure factors for arbitrary rational surface terminations. J. Appl. Crystallogr. 35, 696–701.

van der Zee C., Roberts D. R., Rancourt D. G. and Slomp C. P. (2003) Nanogoethite is the dominant reactive oxyhydroxide phase in lake and marine sediments. Geology 31, 993–996.

Venema P., Hiemstra T., Weidler P. G. and Van Riemsdijk W. H. (1998). J. Colloid Interface Sci. 198, 282–295.

Vlieg E. (2000) ROD: a program for surface X-ray crystallography. J. Appl. Crystallogr. 33, 401–405.

Waychunas G. A., Kim C. S. and Banfield J. F. (2005) Nanoparticulate iron oxide minerals in soils and sediments: unique properties and contaminant scavenging mechanisms. J. Nanopar. Res. 7, 409–433.

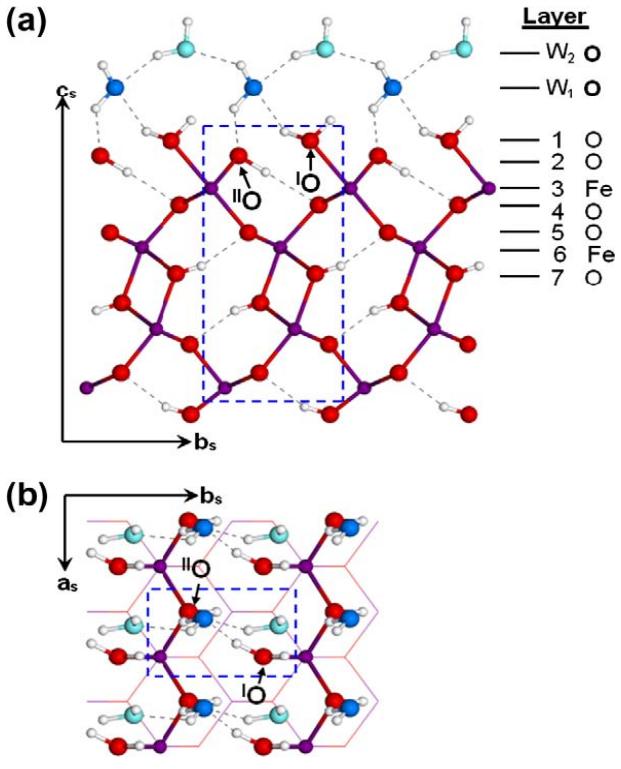

Fig. 1. Atomic structure models for (a) side view of the best fit model: double-hydrated double hydroxyl ((H2O)–(H2O)–OH– OH–Fe–O–O–Fe–R), termination model for the a-FeOOH (100) surface. The atomic symbol and layer sequence in the z-direction are shown. Atoms in bold face represent layers added above the first layer of the stoichiometric termination. A bulk stoichiometric unit cell is shown (dashed box).(b) Top view model of the α-FeOOH(100) surface structure. The large spheres (red) represent oxygen, small spheres (violet) represent iron atoms, and the small spheres (light) represent H atoms. The large spheres in the topmost layer (light blue) and next layer (deep blue), represent the two water layers W2 and W1, respectively. ^{I}O and ^{II}P represent oxygen atoms coordinated to one and two iron atoms, respectively. The plausible hydrogen bonds between the terminal solid surface, and water layers, as well as in the bulk structure, are shown with dashed lines.

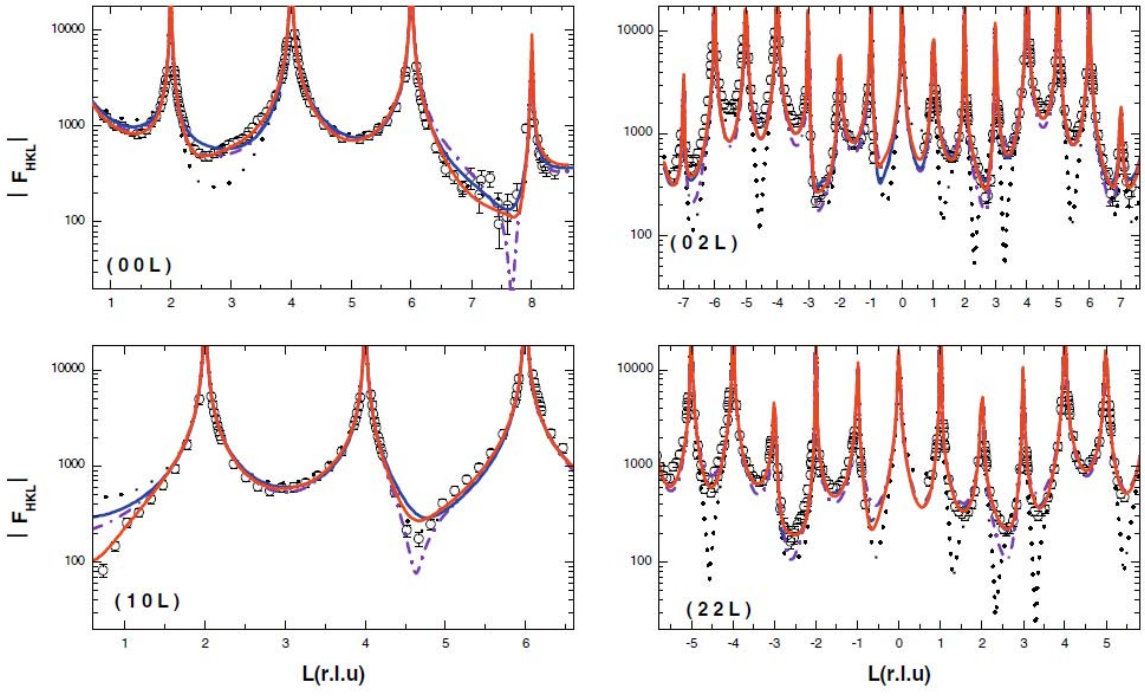

Fig. 2. Selected crystal truncation rods with experimental (circles) and theoretical structure factors (F_{HKL}) as a function of perpendicular momentum transfer (L, in reciprocal lattice units) for the α-FeOOH (1 0 0) surface. The black dotted lines represent calculated CTRs for the unrelaxed left handed double hydroxyl (layer 1) termination (OH–OH–Fe–O–O–Fe–R) model. The violet dash-dotted lines represent calculated CTRs for the relaxed model with equal fractions of the left and right handed double hydroxyl terminations. The blue solid lines are the calculated CTRs for the combined relaxed model with 89% of the surface consisting of the double hydroxyl termination (OH–OH–Fe–O–O–Fe–R). The red solid lines represent the best fit model, utilizing the double-hydrated double hydroxyl terminated model ((H_2O)–(H_2O)–OH–OH–Fe–O–O–Fe–R), where the atoms in bold face represent the water layers.

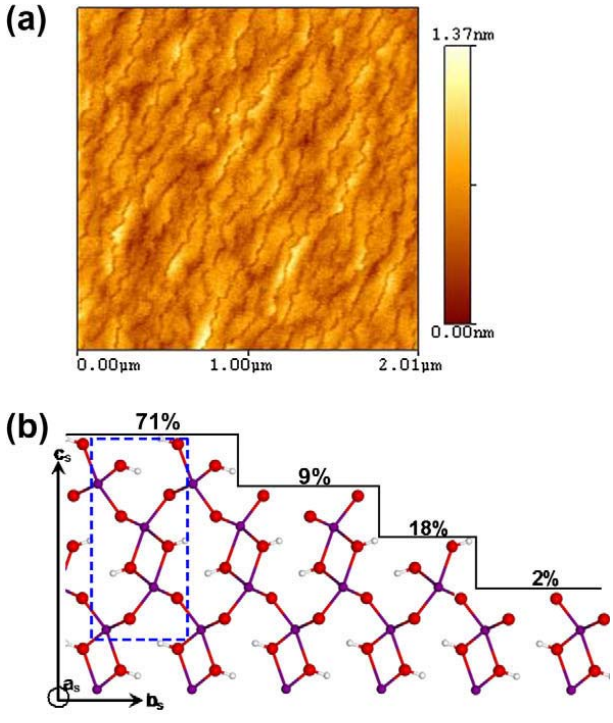

Fig. 3. (a) Step height distributions of goethite (100) surface: AFM image in height mode analysis shown over one 2 µm x 2 µm area, but representative of many such areas. Step height analysis shows the presence of quarter, half, and three quarter step heights. Here a full step height corresponds to the size of the unit cell along the surface normal c_s = 9.9629Å. (b) A schematic representation of the steps on the (1 0 0) surface of the goethite surface model. The blue dashed box shows the unit cell dimensions for a (0 1 1) face. The unequal fractions of different domains are determined from the CTR analysis. The best fit model consists of 71% of double hydroxyl layer 1, 9% double oxygen layer 4, 18% double hydroxyl layer 7 (an opposite handed layer 1)and 2% double oxygen layer 10 (an opposite handed layer 4) with the layer fractions determined with a 2% uncertainty.

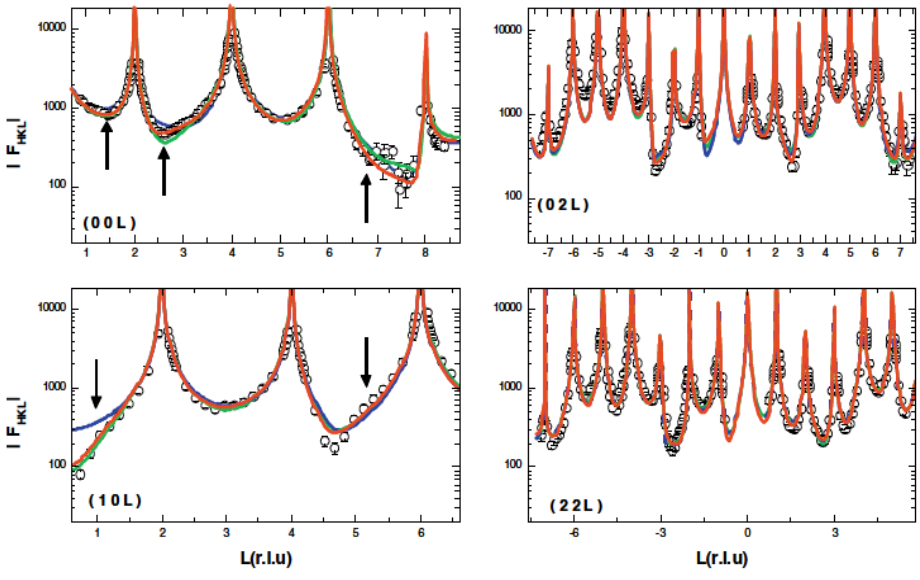

Fig. 4. Selected rods with experimental (circles) and theoretical structure factors(FHKL)as a function of perpendicular momentum transfer (L, in reciprocal lattice units) for the a-FeOOH (100) surface. The blue solid lines are the calculated CTRs for the combined-domain relaxed fit model with double hydroxyl termination (OH–OH–Fe–O–O–Fe–R) with no water layers present. The green solid lines represent the fit model, with single-hydrated double hydroxyl termination ((H_2O)–OH–OH–Fe–O–O–Fe–R). The red solid lines represent the best fit model, the double-hydrated double hydroxyl termination ((H_2O)–(H_2O)–OH–OH–Fe–O–O–Fe–R). The atoms in bold face represent the water layers. The arrows mark the reciprocal lattice positions where the fits have significant mismatch to the experimental data.

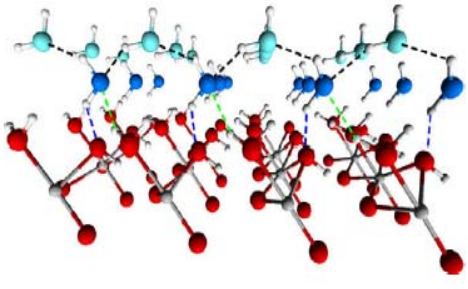

Fig. 5. Three dimensional prospective view (60 degree projected angle) of the interface structural model of hydrated goethite (1 0 0) as derived from the CTR and BV analyses. The view is through the octahedral coordinated crystal interface to the water layers above. Colored dashed lines shows the four hydrogen bonding for the first water layer (W_1) with the terminal hydroxyls and the second water layer (W_2). The dashed colored lines correspond to different hydrogen bond lengths, Green 2.0Å, Black 1.9Å, and Blue 1.7Å.

Table 1. Relaxed and unrelaxed atomic positions and best model fit parameters.

Layers		Unrelaxed surface O—O—Fe—O—O—Fe—R			Relaxed best fit surface (**O—O**)—O—O—Fe—O—O—Fe—R						Predicted model (**H_2O**)—(**H_2O**)—(OH2)—(OH)—Fe—O—O—Fe—R	
		X	*Y*	*Z*	*X*	*Y*	*Z*	B_{iso}(Å^2)	Occp.	$\sum_s$(vu)	Protonation	$\sum_s$(vu)
W_2	**O**				0.40(1)	0.77(8)	1.35(2)	10(2)	0.7(1)		**H_2O**	
W_1	**O**				0.32(5)	0.25(7)	1.21(1)	4(1)	0.7(1)		**H_2O**	
1	^{I}O	0.75	0.803	1.053	0.75	0.66(2)	1.02(1)	2.6(4)	0.81(4)	0.34(6)	H—O—H	1.94
2	^{II}O	0.25	0.197	0.947	0.25	0.15(1)	0.968(3)	0.73	1.0(1)	0.82(4)	H. . .O—H	1.82
3	Fe	0.75	0.951	0.854	0.75	0.82(4)	0.853(2)	0.63	0.79(2)	2.95(4)	Fe	2.95
4	O	0.25	0.705	0.800	0.25	0.956(4)	0.795(3)	0.73	1.00	1.82(4)	O. . .H	2.02
5	O	0.75	0.205	0.700	0.75	0.72(1)	0.698(3)	0.73	1.00	1.84(4)	Fe	2.04
6	Fe	0.25	0.451	0.646	0.25	0.22(1)	0.645(1)	0.63	1.00	3.06(3)	Fe	3.06
7	O	0.75	0.697	0.553	0.75	0.452(3)	0.553(2)	0.73	1.00	1.19(2)	O—H	1.99
8	O	0.25	0.303	0.447	0.25	0.697	0.446(2)	0.73	1.00	1.19(2)	O—H	1.99
9	Fe	0.75	0.549	0.354	0.75	0.303	0.354	0.63	1.00	2.97(1)	Fe	2.97
10	O	0.25	0.796	0.300	0.25	0.549	0.300	0.73	1.00	1.78	O. . ...H	1.98
11	O	0.75	0.296	0.200	0.75	0.796	0.200	0.73	1.00	1.78	O. . ...H	1.98
12	Fe	0.25	0.049	0.146	0.25	0.296	0.146	0.63	1.00	2.96	Fe	2.96
13	O	0.75	0.803	0.053	0.75	0.049	0.053	0.73	1.00	1.18	O—H	1.98

Fractional coordinates ($a = 3.0231$ Å, $b = 4.6088$ Å, $c = 9.9629$ Å) of atoms in the surface model for unrelaxed double hydroxyl termination (bulk) and best fit relaxed surface. Estimated errors from the least-squares fit at the 95% confidence level are given in parentheses. Values without reported errors were held fixed in the fits. Bond-valence sum ($\sum_s$) values in Valence Unit (vu) were calculated according to the method described in the text. Protonation for the best fit model and the resulting BV sums, as well as for all layers in the bulk are also reported.